Missouri University of Science and Technology
Scholars' Mine

Mechanical and Aerospace Engineering Faculty Research & Creative Works

Mechanical and Aerospace Engineering

05 Aug 2009

Development of Extrusion-on-Demand for Ceramic Freeze-Form Extrusion Fabrication

Thomas Oakes

Parimal Kulkarni

Robert G. Landers
Missouri University of Science and Technology, landersr@mst.edu

Ming-Chuan Leu
Missouri University of Science and Technology, mleu@mst.edu

Follow this and additional works at: https://scholarsmine.mst.edu/mec_aereng_facwork

 Part of the Manufacturing Commons

Recommended Citation

T. Oakes et al., "Development of Extrusion-on-Demand for Ceramic Freeze-Form Extrusion Fabrication," *Proceedings of the 20th Annual International Solid Freeform Fabrication Symposium (2009, Austin, TX)*, pp. 206-218, University of Texas at Austin, Aug 2009.

This Article - Conference proceedings is brought to you for free and open access by Scholars' Mine. It has been accepted for inclusion in Mechanical and Aerospace Engineering Faculty Research & Creative Works by an authorized administrator of Scholars' Mine. This work is protected by U. S. Copyright Law. Unauthorized use including reproduction for redistribution requires the permission of the copyright holder. For more information, please contact scholarsmine@mst.edu.

DEVELOPMENT OF EXTRUSION-ON-DEMAND FOR CERAMIC FREEZE-FORM EXTRUSION FABRICATION

Thomas Oakes, Parimal Kulkarni, Robert G. Landers, and Ming C. Leu

Department of Mechanical and Aerospace Engineering

Missouri University of Science and Technology,

Rolla, MO 65409

{tmo6w3@mst.edu, pskf44@mst.edu, landersr@mst.edu, mleu@mst.edu }

{Oakes: (573) 341-4862, Kulkarni: (573) 263-5949, Landers: (573) 341-4586, Leu: (573) 341-4482}

ABSTRACT

In the Freeze-form Extrusion Fabrication (FEF) process, extrusion-on-demand (EOD) refers to the ability to control the start and stop of paste extrusion on demand and is vital to the fabrication of parts with complex geometries. This paper describes the development of EOD for ceramic FEF through modeling and control of extrusion force, selection of appropriate process parameters, and a dwell technique for start and stop of extrusion. A general tracking controller with integral action is used to allow tracking of a variety of reference forces while accounting for the variability in the paste properties. Experiments are conducted to model the process and tune the controller. The developed technique for EOD is demonstrated to fabricate a number of cross sections and three-dimensional parts from alumina paste.

1. INTRODUCTION

Fabricating ceramic materials into usable 3D components is a complicated, costly, and time-consuming process that usually involves pressing ceramic powder to near net shape, sintering, and finish machining or diamond grinding of the final geometry from a block of dense ceramic. Using organic or aqueous based slurries, cast into a prefabricated mold designed to mimic the shape of the final product, is another method for fabricating 3D ceramic components. After casting, the green form undergoes binder removal and sintering to produce a dense ceramic product. The cost and time associated with mold design and processing tend to increase greatly with geometric complexity of the component. Further, a mold-based fabrication process cannot produce 3D components with internal passages and cavities. In recent years, several Solid Freeform Fabrication (SFF) techniques have been developed to fabricate 3D ceramic components, including Fused Deposition of Ceramics [1], Fused Deposition Modeling [2], Extrusion Freeform Fabrication [3], 3D Printing [4], Selective Laser Sintering [5,6], Selective Laser Melting [5], Shape Deposition Manufacturing [7], and Robocasting [8,9]. All of these techniques involve layer-by-layer material addition. Most of them produce a nearly finished product (after sintering) without a mold, while some others involve fabricating a mold or 3D tooling to form the final component by casting.

Especially relevant to the research in the present paper are the Extrusion Freeform Fabrication (EFF) and Robocasting processes. EFF is the first SFF process in utilizing extrusion of organic pastes to build 3D ceramic components [3]. Robocasting is the first SFF process that extruded aqueous pastes to fabricate parts from ceramics [8,9]. The use of aqueous based extrusion has several unique advantages: (1) it is environmentally friendly; (2) its minimal amount of organic binder reduces time for binder pyrolysis; (3) its equipment cost is low compared with laser based and other SFF processes; and (4) the process can easily accommodate use of multiple materials to make functionally graded components.

EFF and Robocasting are room temperature SFF processes. Due to the intrinsic properties of ceramic pastes in room temperatures, deformation (slumping) of large parts during the fabrication process cannot be avoided. One way to remedy this is to solidify the paste rapidly in a freezing environment after it is extruded. This can be accomplished by extruding aqueous pastes at temperatures below the freezing point of the aqueous medium. This is the basis of the Freeze-form Extrusion Fabrication (FEF) process, which extrudes aqueous ceramic paste of high solids loading in a layer-by-layer manner for part fabrication. The FEF process has been demonstrated for fabrication of ceramic parts by continuous extrusion of aqueous paste [10,11].

The FEF study described in the present paper uses ceramic paste made of alumina (Al_2O_3) powder, water, dispersant, lubricant and other materials. The ceramic solids loading is up to 50 vol.% of the paste. Water is the main liquid medium, with the organic binder content only 2–4 vol.%. A ram extruder mechanism is used to extrude the paste. The extruder is mounted on a 3D gantry system. The experimental setup is shown in Figure 1. The green part obtained after fabrication is freeze-dried, the binder is removed through a burnout process, and the brown part is then sintered to obtain the final part.

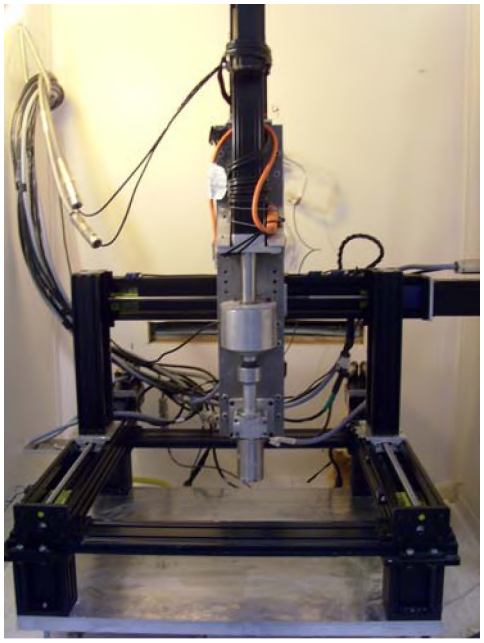

Figure 1: Experimental setup with an extruder ram mounted on a 3D gantry system

Control of the paste flow rate, extrudate consistency, and start and stop of extrusion as prescribed is a major challenge in the FEF process development. This requires understanding of the paste dynamics. Benbow and Bridgewater [12] developed an equation relating the extrusion pressure to the paste velocity during steady-state extrusion, with the assumption that the paste is incompressible and undergoes slip in the die land. Mason et al. [13] conducted an empirical study on the dynamics of the paste and showed that the paste flow can be modeled as a first-order system with significant variations in the gain and time constants. Amarasinghe and Wilson [14] stated that ceramics are generally much more difficult to extrude as compared to polymers due to temporal and spatial inconsistencies in the paste properties. Another study investigated the use of a bang-bang control strategy with feedback control of the extrusion force [15]. Drawbacks of this control technique include excessive use of trial and error and lack of systematic protocols. Zhao et al. [16] successfully conducted continuous extrusion fabrication with an adaptive controller to regulate the extrusion force. However, the resulting parts were limited to shapes that could be made with continuous extrusion. Another study by Mason et al. [17] investigated start and stop of extrusion in conjunction with force control. This paved the initial path for the extrusion-on-demand extrusion study presented in the present paper.

The objective of this paper is to develop a force controller that is capable of extrusion-on-demand for the FEF process. The rest of the paper is organized as follows. In Section 2, the FEF experimental setup and process modeling are described. Next, in Section 3, the dynamic paste extrusion model is used to design a general tracking controller with integral action to account for paste variability. The main FEF process parameters are introduced in Section 4, along with the acceptable ranges of these parameters determined experimentally. The fabrication of 2D cross-sections and 3D parts with the developed extrusion-on-demand FEF process is described in Section 5. Finally, a conclusion of the study is given in Section 6.

2. PROCESS MODELING

A series of tests are conducted to obtain a dynamic model for the FEF extrusion process. The input is set to an upper bound voltage (250 mV) until the start of extrusion has occurred as is visually confirmed. Once extruding, the system is subjected to a series of step changes in the command voltage which is cycled several times. Plots of the response and input are shown in Figure 2.

A dynamic first order model of the FEF process is

$$G(z) = \frac{F(z)}{U(z)} = \frac{b(z)}{a(z)} = \frac{b_0}{z + a_0} \tag{1}$$

where b and a are model coefficients to be determined through a recursive least squares algorithm. Equation (1) is transformed into the difference equation

$$F(i) = -aF(i-1) + bU(i-1) \tag{2}$$

The recursive least squares (RLS) algorithm is implemented with

$$\varphi = \begin{bmatrix} -F(i-1) & U(i-1) \end{bmatrix}^T \tag{3}$$

$$\eta = \begin{bmatrix} a_0 & b_0 \end{bmatrix}^T \tag{4}$$

where $a_0 = -0.998$ and $b_0 = 0.0397$, which are determined empirically based on the RLS algorithm. Equation (1) is thus

$$G(z) = \frac{K(1-b)}{z - \exp(-T/\tau)} = \frac{0.0397}{z - 0.998} \tag{5}$$

where $K = 0.0413$ kN/mV, $T = 0.1$ s is the sample period, and $\tau = 42.7$ s is the time constant. The model is used to plot against the data collected from the experiment as shown in Figure 2. The good agreement indicates that the first-order process approximation is acceptable to describe the process dynamics and can be used for controller design.

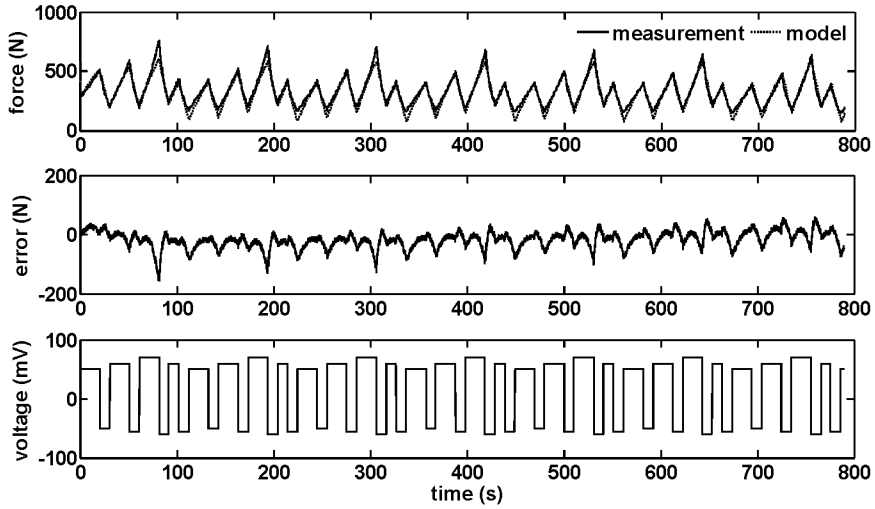

Figure 2: Comparison of measurement data with modeled response for the given input profile

To find the relationship between ram extrusion force and extrudate velocity at steady state, a series of tests are conducted to collect values of steady-state extrudate

velocity at constant ram extrusion forces. Based on the experimental data, the force-velocity relationship is approximately linear over the range of forces used in the experiment. A least squares regression results in the following relationship:

$$V_{ext} = 0.043F - 7.403 \tag{6}$$

where V_{ext} is the extrudate velocity in m/s. The regression yields $R^2 = 0.857$, indicating an acceptable correlation.

3. CONTROLLER DESIGN

A control algorithm is designed to allow for extrusion on demand of the FEF process in order to extrude the paste at a constant rate and to coordinate the start of extrusion with the gantry motion. This algorithm uses the general tracking control to reject constant disturbances with desired error dynamics

$$[v(z)a(z) - g(z)]E(z) = 0 \tag{7}$$

where *v(z)* is the disturbance generating polynomial and is

$$v(z) = z - 1 \tag{8}$$

and E(z) is the controller error and is

$$E(z) = R(z) - F(z) \tag{9}$$

where R(z) is the reference ram extrusion force and F(z) is the measurement from the load cell. a(z) is the denominator of the open-loop transfer function, and g(z) is a first-order polynomial

$$g(z) = g_1 z + g_0 \tag{10}$$

where g_1 and g_0 are determined by the desired closed-loop error dynamics. Equation (7) can be rewritten as

$$[z^2 + (a - 1 - g_1)z + (-a - g_0)]E(z) = 0 \tag{11}$$

In order to allow the system to exhibit a first-order response, one of the poles in the control system is suppressed by making the second pole at least one order of magnitude smaller than the dominant pole. The dominant pole is selected in order to decrease the settling time as much as possible without causing system instability. Two overdamped poles are thus selected with time constants $\tau_1 = 1.5$ s and $\tau_2 = 0.15$ s. The desired closed-loop characteristics are represented by the following polynomial

$$z^2 - 1.449z + 0.480 = 0 \tag{12}$$

Equating the characteristic polynomials in equations (10) and (12), we obtain $g_1 = -0.549$ and $g_2 = 0.517$. The control signal is related to the reference and error signals by

$$v(z)b(z)U(z) = v(z)a(z)R(z) - g(z)E(z) \tag{13}$$

Equation (13) is expanded and discretized to solve for the control signal at iteration *i*

$$U(i) = U(i-1) + \frac{1}{b}[R(i+1) + (a-1)R(i) - aR(i-1) - g_1E(i) - g_0E(i-1)] \tag{14}$$

Equation (14) is coded into the Delta Tau controller language and implemented with a step reference force of 178 N for validation. The controller tracks a step reference with an approximate settling time of 18 s. This response time is much too slow for extrusion on demand so the controller is implemented again with the reference force ramped to decrease the settling time. The result is shown in Figure 3, which demonstrates that the controller tracks the ramp reference with an approximate settling time of 5 s. Thus using a ramp reference force rather than a step reference force has decreased the response time by a factor of more than 3. It should be noted that the controller does not

saturate throughout the test due to smaller changes in the error. The pulsing of the ram caused by the constant over and under correction during the ramp input probably excites the paste into a faster response. From this point forward, all reference forces are set to ramp to the desired values with the same slope.

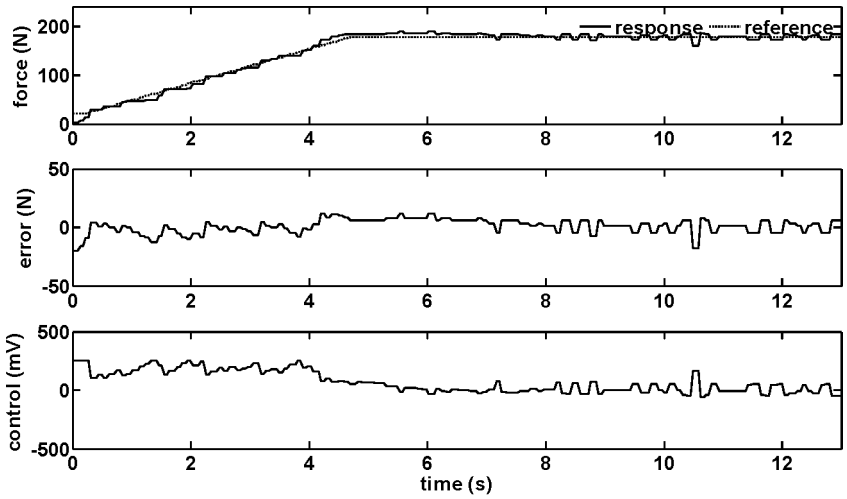

Figure 3: Response of ram extrusion force for a ramp input

The controller is subjected to a variety of changes in the reference force to compare their effects on variation in the control signal and, as a result, the ram velocity required to maintain different reference forces. It has been experimentally established that reference forces greater than 535 N will result in controller instability.

4. PROCESS PARAMETERS

The quality of the FEF process is affected by many process parameters including the table velocity, ram velocity, dwell periods, standoff distance, overlap factor, and environmental and heating temperatures. This section discusses these parameters and a series of experiments conducted to determine the ranges of working values for these parameters for the extrusion-on-demand FEF process. The nozzle diameter for all experiments is 580 microns.

4.1. Ram Velocity

The ram velocity is controlled directly by the command input voltage and is constantly updated online to regulate the extrusion force. The ram velocity and the command input voltage are positively correlated, implying that the ram velocity and the extrusion force are also positively correlated. In general, a constant ram velocity produces a fairly constant force, but only if the paste has already begun to extrude out of the nozzle. The ram velocity continuously oscillates to maintain a constant force. In general, the average ram velocity over a period of steady-state force control has a slightly positive bias, generally in the order of μm/s.

4.2. Table Velocity

The magnitude of the table velocity should be set equal to the magnitude of the extrudate velocity, which is the velocity of the paste as it exits the nozzle, to ensure that paste is distributed uniformly. Equation (6) empirically relates the average extrudate velocity to the average input ram force. This relationship implies that a constant force input will result in a constant extrudate velocity, and that the two are positively correlated. However, a point exists at which there is not enough force to cause extrusion. Table velocities that are too high with respect to the extrudate velocity will result in thin and sometimes incomplete paste deposition, thus forming voids. On the other hand, table velocities that are too low result in excessive deposition per unit length, causing surface defects from dragging the nozzle and forming thick, non-uniform lines.

4.3. Standoff Distance

Standoff distance refers to the distance between the nozzle tip and the top of a previously deposited layer (or substrate). It is expressed as percentage of the measured extrudate diameter. A standoff distance that is too low will result in thick extrusion containing a surface defect due to the nozzle dragging through the previously deposited layers, possibly resulting in part collapse. A standoff distance that is too high will result in discontinuous or thin lines during extrusion due to lack of contact between the paste and surface, eventually leading to uncontrolled deposition and part collapse.

Prior to determining a working range of standoff distance, the extrudate diameter must be determined. This is accomplished by photographing the extrudate during steady-state extrusion and pixel comparison of the photograph. The experiment is conducted over constant ram extrusion forces ranging between 350 N to 500 N in increments of 25 N. The average extrudate diameter is calculated to be 617 μm with a standard deviation of 6.44×10^{-2} μm.

Single line testing is not reliable in this case because inappropriate standoff distances are generally not made apparent until several layers have been deposited. A series of four hollow cylinders 25.4 mm in height and 25.4 mm in diameter are fabricated at the ram extrusion force of 450 N and the table velocity of 4.87 mm/s. The tested standoff distances are 70%, 55%, 40%, and 25% of the extrudate diameter, and the result is shown in Figure 4. The standoff distance at 70% is too high for good layer consistency. The parts fabricated at 55% and 40% both appear to have good layer consistency and surface finish. The cylinder fabricated at the standoff distance of 25% of extrudate diameter contains no air gaps, but is visually much thicker than the rest of the specimens. The established range of standoff distances is thus between 40% and 55% of the extrudate diameter.

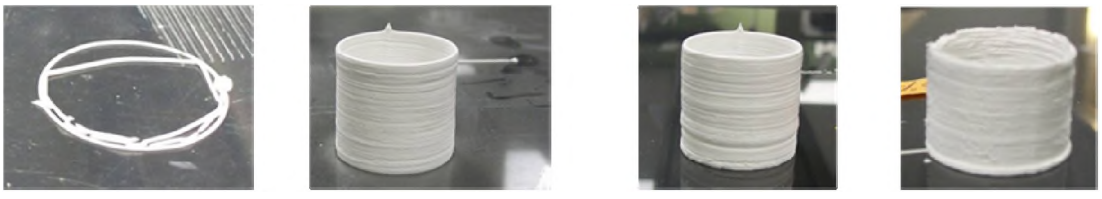

Figure 4: Testing of four standoff distances: 70%, 55%, 40%, and 25% of the extrudate diameter

4.4. Overlap Factor

The overlap factor refers to the spacing between two neighboring lines and is defined as

$$K_{OL} = \frac{-d_{gap}}{D_{ext}} \tag{15}$$

where D_{ext} is the extrudate diameter and d_{gap} is the gap between two neighboring deposited lines. An overlap factor of zero implies that the centers of two successive parallel lines are exactly one extrudate diameter apart. A positive overlap factor implies that the line centers are closer than the extrudate diameter, which can lead to accumulation of material and undesirable part quality. A negative overlap factor implies that the line centers are further apart than one extrudate diameter. Parts with excessive negative overlap factors will have voids between extruded lines, which may lead to poor structural integrity and will ultimately lead to the part collapse.

A series of single-layered plate, 25.4 mm x 35.6 mm, are fabricated at a standoff distance of 55% of the extrudate diameter to determine the working range of the overlap factor. All tested values of overlap factor are negative due to the compaction of deposited material caused by the low standoff distance (55% of the extrudate diameter). Values tested are -60%, -45%, -30%, and -15% with three cross-sections fabricated per overlap factor. The result is shown in Figure 5. Rastered parts at -60% contain visual voids in the rastering structure. Parts created at -15% contains slight accumulation of materials between deposited lines, implying the spacing is too close. Overlap factors of -45% and -30% both exhibit acceptable raster quality.

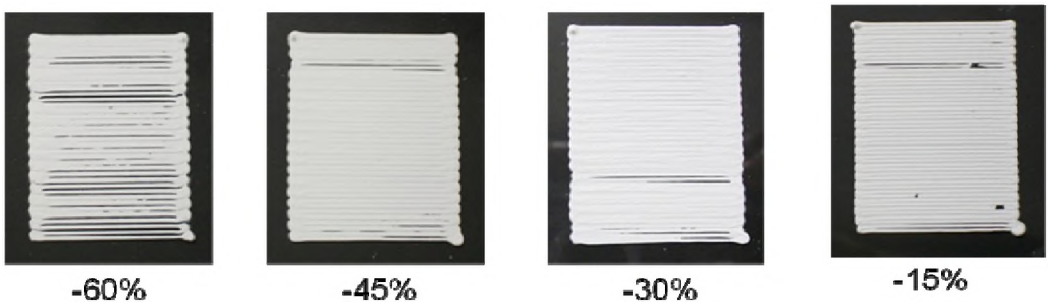

Figure 5: Testing of four (4) overlap factors: -60%, -45%, -30%, and -15% of the extrudate diameter; standoff distance = 55% of the extrudate diameter

4.5. Dwell Time for Start and Stop

Determining the dwell time at the start and stop of extrusion is important for extrusion-on-demand (EOD). Dwell time refers to the amount of time required for the gantry to remain stationary after the force controller is activated for paste extrusion. Excessive dwell times at the start cause material accumulation at the beginning of the line and can lead to nozzle clogging. Dwell times that are too short at the start may cause the deposition head to begin advancing along the path prior to extrusion of paste, leading to incomplete deposition lines.

Start dwell time is set as a function of the reference ram force. The gantry is allowed to advance along its path after a specified force (in percentage of the reference

ram force) is attained by the force controller. Stop dwell time is simply set to three seconds, in which the gantry movement is terminated followed by the ram retraction at the maximum motor speed prior to activation of the next motion command.

Since the start dwell time is a function of the extrusion force, it is also a function of the extrudate velocity (which is also the table velocity). Good EOD is hard to achieve at high speeds, and the performance of the start and stop technique improves as the velocity/force is decreased. However, operating at a very low velocity/force combination is not recommended due to potential for discontinuous extrusion and nozzle clogging besides low productivity.

The start dwell time for the FEF process is analyzed through a series of extrusion line tests. The reference extrusion force is varied from 350 to 500 N in 25 N increments at a standoff distance equal to 55% of the extrudate diameter for each test. During each test, five 127 mm lines are extruded at dwell times ranging from 50% to 70% in 5% increments of the reference ram force. The result is shown in Figure 6, which depicts that the amount of excess material accumulation during the dwell period decreases as the reference extrusion force decreases. This implies that a low ram force should be used for extrusion; however, a low force does not guarantee continuous extrusion over time. In most cases, lines deposited with dwell times set at less than 65% of the extrusion force are discontinuous. All lines deposited with dwell times set at larger than 70% of the extrusion force display moderate to severe tapering. The start dwell time is thus established between 65% and 70% of the reference extrusion force.

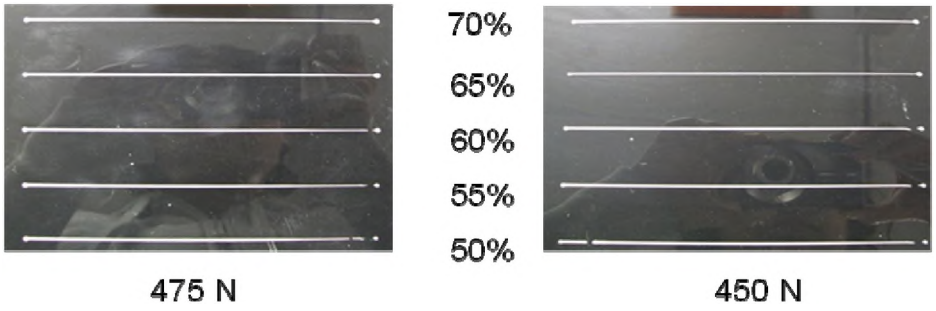

Figure 6: Lines deposited with the start dwell time ranging from 50% to 70% in 5% increments of the reference extrusion force

4.6. Environmental and Paste Temperatures

The environmental temperature refers to the temperature of the freezer in which the gantry system is contained. Liquid nitrogen is dispersed in streams aimed at the substrate, keeping the environment temperature at -5 °C around the build area. As the environmental temperature decreases, the process allows for faster freezing of deposited material and higher part stability. Temperatures that are too low may result in nozzle clogging due to freezing of paste in the die land. Increased environmental temperatures allow for higher extrudate velocities at lower forces, but reduce part stability due to insufficient freezing of deposited lines.

The paste temperature refers to the temperature of the paste maintained by the heating tape around the sleeve of the stainless steel syringe. Low paste temperatures may result in partial freezing of the paste inside the syringe, preventing extrusion at lower

forces. High paste temperatures change the paste consistency, making it more difficult to quick freeze the extrudate. The paste temperature is fixed at 10 °C in this study.

5. PART FABRICATION

Experiments are conducted to fabricate 2D cross-sections and 3D parts by the FEF process requiring EOD. The process parameters used for the fabrication are: table velocity = 4.87 mm/s, standoff distance = 55% of the extrudate diameter, dwell time = time arriving at 70% of the reference ram extrusion force, and overlap factor = -45% of the extrudate diameter.

Insight 4.3.1 software is used to slice .stl files into sections and generate extrusion paths based on the selected process parameters. The layer and generated tool path of a simplified fuel injector strut is shown in Figure 7. The part is scaled to 7.62 mm x 50.8 mm x 25.4 mm and oriented such that the larger dimensions are on the x-y plane, in order to minimize the build height.

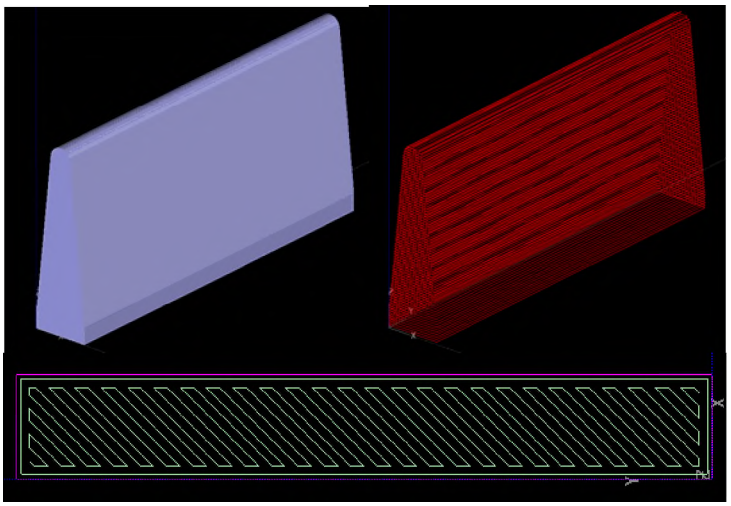

Figure 7: Generation of layers and tool paths using Insight

The fuel injector strut's cross sections are deposited in a side-by-side manner first to test the viability of continuous extrusion between commanded deposition starts and stops. Each layer contains two starts and stops, the first for contouring and the second for internal rastering. The results are shown in Figure 8. The experimental setup is capable of continuous extrusion over all layers. Material accumulation is observed at all points of initial deposition, implying that stacking of these layers could result in a height offset which would interfere with the standoff distance. The second cross-section down from the top right contains a void due to an air gap in the syringe.

Layers of alumina paste are deposited and stacked to fabricate a simplified fuel injector strut. Successive layers are oriented 90° apart to improve the structural stability. Figure 9 shows four of these parts fabricated by the process.

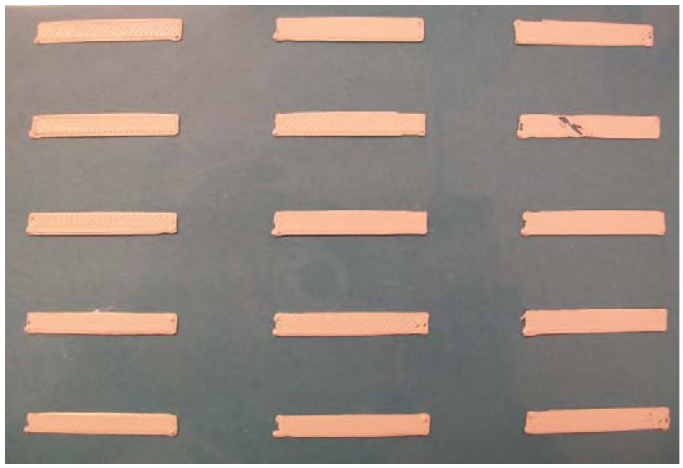

Figure 8: Extrusion of 15 cross-sections of a simplified fuel injector strut

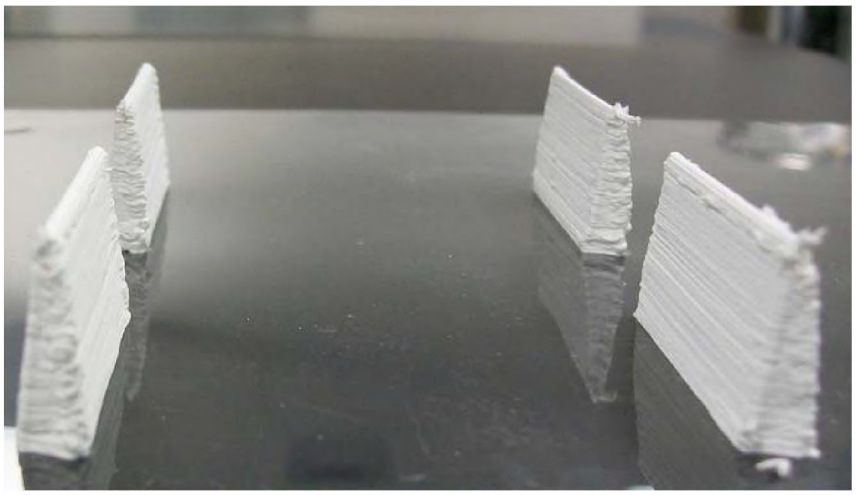

Figure 9: Simplified fuel injector struts fabricated by the FEF process

6. CONCLUSIONS

Working ranges have been established for FEF of aqueous alumina paste for the following process parameters: table velocity, ram velocity, standoff distance, dwell time, overlap factor, environmental temperature, and paste temperature. Extrusion on demand has been made possible through the implementation of a general tracking controller with appropriate start and stop dwell times at the beginning and end of a continuous extrusion path. Successful 2D cross sections and 3D parts have been fabricated using the FEF process with the developed EOD control technique. Further study of the extrudate velocity profile along the extrusion path will also be needed in order to eliminate excess accumulation of material at the beginning of extrusion.

7. ACKNOWLEDGMENTS

This research was supported by the U.S. Air Force Research Laboratory through the Center for Aerospace Manufacturing Technologies (CAMT), contract #FA8650-04-C-5704, at the Missouri University of Science and Technology (Missouri S&T), and by

CAMT Industrial Consortium whose members consist of Boeing, General Dynamics, Spirit AeroSystems, GKN Aerospace, Siemens, KMT Waterjet, the Product Innovation and Engineering, Spartan Light Metal Products, and the Third Wave Systems. The research was also supported by Missouri S&T's Intelligent Systems Center. Special thanks are due to Drs. G. E. Hilmas and T. Huang for expert advice on alumina paste preparation and post processing.

8. REFERENCES

[1] Bandyopadhyay, A., Panda, P. K., Agarwala, M.K., Danforth, S.C., and Safari, A., "Processing of Piezocomposites by Fused Deposition Technique," Journal of the American Ceramic Society, Vol. 80, No.6, pp. 1366-1372 (2000).

[2] Crump, S.S., "Appartus and Method for Ceramic Three-Dimensional Objects," U.S. Patent No. 5121329 (1992).

[3] Hilmas, G.E., Lombardi, J.L., and Hoffman, R.A., "Advances in the Fabrication of Functional Graded Materials using Extrusion Freeform Fabrication," Functionally Graded Materials, Proceedings of Solid Freeform Fabrication Symposium, Austin, TX, pp. 319-324 (1996).

[4] Cima, M.J., Oliveira, M., Wang, H.R., Sachs, E., and Holman, R., "Slurry-Based 3DP and Fine Ceramic Components," Proceedings of Solid Freeform Fabrication Symposium, Austin, TX (2001).

[5] Kruth, J.P., Mercelis, P., Froyen, L., and Rombouts, M., "Binding Mechanisms in Selective Laser Sintering and Selective Laser Melting," Proceedings of the Solid Freeform Fabrication Symposium, Austin, TX (2004).

[6] Leu, M. C., Adamek, E. B., Huang, T., Hilmas, G. E., and Dogan, F., "Freeform Fabrication of Zirconium Diboride Parts Using Selective Laser Sintering," Proceedings of Solid Freeform Fabrication Symposium, Austin, TX (2008).

[7] Stampfl, J., Cooper, A., Leitgeb, R., Cheng, Y., and Prinz, F., "Shape Deposition Manufacturing of Microscopic Ceramic and Metallic Parts Using Silicon Molds," U.S. Patent, No. 6242163 (2001).

[8] Cesarano, J. III, Segalmen, R. and Calvert, P., "Robocasting Provides Moldless Fabrication from Slurry Deposition," Ceramics Industry, Vol. 148, pp. 94-102 (1998).

[9] He, G., Hirschfeld, D. A., Cesarano, J., III, Stuecker, J. N., "Processing of Silicon Nitride-Tungsten Prototypes." Ceramic Transactions, Vol. 114, pp. 325-332 (2000).

[10] Huang, T. S., Mason, M., Hilmas, G., and Leu, M.C., "Freeze-form Extrusion Fabrication of Ceramic Parts," International Journal of Virtual and Physical Prototyping, Vol. 1, No. 2, pp. 93-100 (2006).

[11] Huang, T. S., Mason, M., Hilmas, G., and Leu, M.C., "Aqueous Based Freeze-form Extrusion Fabrication of Alumina Components," Rapid Prototyping Journal, Vol. 15, No. 2, pp. 88-95. (2009).

[12] Benbow, J. J., and Bridgwater, J., "Paste Flow and Extrusion," Clarendon Press, Oxford (1992).

[13] Mason, M.S., Huang, T.S., Landers, R.G., Leu, M.C., and Hilmas, G.E., "Freeform Extrusion of High Solids Loading Ceramic Slurries, Part I: Extrusion Process Modeling," Seventeenth Annual Solid Freeform Fabrication Symposium, Austin, Texas (2006).

[14] Amarasinghe, A.D.U.S. and Wilson, D.I., "Interpretation of Paste Extrusion Data," Chemical Engineering Research and Design, 76(A1), pp. 3–8 (1998).
[15] Mason, M.S., Huang, T.S., Landers, R.G., Leu, M.C., and Hilmas, G.E., "Freeform Extrusion of High Solids Loading Ceramic Slurries, Part II: Extrusion Process Control," Seventeenth Annual Solid Freeform Fabrication Symposium, Austin, Texas (2006).
[16] Zhao, X., Landers, R.G., and Leu, M.C., "Adaptive Control of Freeze–form Extrusion Fabrication Processes," ASME Dynamic Systems and Controls Conference, Ann Arbor, Michigan (2008).
[17] Mason, M.S., Huang, T., Leu, M.C., Landers, R.G., and Hilmas, G.E., "Aqueous–Based Extrusion Fabrication of Ceramics on Demand," Eighteenth Annual Solid Freeform Fabrication Symposium, Austin, Texas (2007).